Journal of Materials and Environmental Sciences
ISSN : 2028-2508
CODEN : JMESCN

J. Mater. Environ. Sci., 2019, Volume 10, Issue 2, Page 101-112

http://www.jmaterenvironsci.com

Study of Green Corrosion Inhibition on AISI 1018 Carbon Steel in Sulfuric Acid Using *Crataegus mexicana* as Eco-Friendly Inhibitor.

A. Rodríguez-Torres[1], M. G. Valladares-Cisneros[2*], C. Cuevas-Arteaga[3], M. A. Veloz-Rodríguez[1]

[1]*Área Académica de Ciencias de la Tierra y Materiales. Instituto de Ciencias Básicas e Ingeniería. Universidad Autónoma de Estado de Hidalgo. 42186, Pachuca de Soto, Hgo, México*

[2]*Facultad de Ciencias Químicas e Ingeniería, Universidad Autónoma del Estado de Morelos, Av. Universidad 1001, Chamilpa, C.P. 62209, Cuernavaca, Morelos, México.*

[3]*Centro de Investigación en Ingeniería y Ciencias Aplicadas, Universidad Autónoma del Estado de Morelos, Av. Universidad 1001, Chamilpa, C.P. 62209, Cuernavaca, Morelos, México.*

Received 22April 2019,
Revised 25 April 2019,
Accepted 25 April 2019

Keywords
- ✓ *Crataegus Mexicana,*
- ✓ Green corrosion inhibition,
- ✓ Eco-friendly inhibitor,
- ✓ AISI 1018 carbon steel,
- ✓ Sulfuric acid.

mg.valladares@uaem.mx;
Phone: +527773297039;
Fax: +527773297039

Abstract

Green corrosion inhibition on AISI 1018 carbon steel immersed in 0.5M H_2SO_4 by *Crataegus mexicana* is develop using Electrochemical Impedance Spectroscopy (EIS), Potentiodynamic Polarization Curves (PPC) and weight loss method. The metal surface morphology was analysed by Scanning Electron Microscope (SEM). And the chemical characterization of eco-friendly inhibitor is carried out by Fourier Transform Infrared (FTIR). The EIS showed that the use of 500 ppm of methanol extract of *C. mexicana* allow reaches 80% of corrosion inhibition efficiency (CIE). Through PPC of CIE obtained was 75 % and *C. mexicana* acts a mix type inhibitor. The CIE obtained by weight loss method was 95% for the eco-friendly inhibitor. The adsorption of *C. mexicana* over metal surface obeys the Frumkin isotherm and according to the Gibbs free energy the eco-friendly inhibitor acts by physisorption process. The FTIR shows the characteristic signals of the functional groups present in flavonoids. The *Lactuca sativa* seeds toxicity bioassay shown that *C. mexicana*is slightly toxic to the bioindicator organism.

1. Introduction

Acid solutions are commonly used in industry where hydrochloric and sulfuric acids are the most used to remove iron oxides that are formed in the steel [1]. Over time, the frequent use of these acid solutions may cause deterioration in metallic materials. Nowadays, the industry and the academic sectors have been interested in the use of inhibitors due to their adsorption onto the metal surface can reduce the corrosion rate, such adsorption depends on the physical-chemical properties of the inhibitor molecules, the metal nature, the aggressiveness of the corrosive medium, the temperature and the electrochemical potential in the metal-solution interface [2]. By the other hand, the legislations and environmental policies enforce restrictions and the installation of residual water treatment plants as a cause of toxic inhibitors, which cause an increment in costs for industries [3]. Those circumstances motivate the increase in developing effective and low toxicity chemical substances daily. Natural organic molecules such as caffeine [4], tryptamine and succinic acid [5] have been reported as good inhibitors that are absorbed onto the metal surface decreasing the corrosion rate. The mechanism of the inhibitor is attributed to the presence of polar functions with N and O atoms and π electrons [6] into their chemical heterocyclic structures of these organic compounds.

Due to this fact the interest in developing green inhibitors was increased reporting a good corrosion inhibition efficiency in the inhibitors obtained from plants in acid media [7]. Some corrosion inhibitors have been reported: *Equisetum arvense* [8], Mentha pulegium [9], *Thymus algeriensis* [10], *Thymus vulgaris* [11], *Pancratium foetidum* [12], *Lavandula pedunculata* [13], *Rollinia occidentalis* [14], *Pithecollobium dulce* [15], and Allicine [16] from garlic [17].

The used of almond leaves extract as corrosion inhibitor on Aluminum immerse in 1 M HCl revealed that 0.38 g L^{-1} of it given 97.9 % of corrosion inhibition efficiency [18]. Cherry sticks was explored as corrosion inhibitor on mild steel in 1M of HCl, the results revealed that 0.5 g L^{-1} reach a 89.5 % of corrosion inhibition

efficiency [19]. *Equisetum arvense* decreased the corrosion rate on A36 steel in 0.5 M sulfuric acid about two orders of magnitude and increase the polarization resistance and a greater efficiency of inhibition by increasing the concentration of extract [8].

Recently was studied the inhibitive effect of *Crataegus oxyacantha* (hawthorn) and *Prunus avium* (sweet cherry) leave extracts on the corrosion of mild steel in hydrochloric acid solution. Both acted as mixed type green inhibitors and adsorption took place through physisorption mechanism and the corrosion inhibition efficiency was close to 60 % [20].*Prunus persica* leaves was studied as a green corrosion inhibitor of AISI 1018 carbon steel in 0.5 M H_2SO_4, the corrosion inhibition efficiency was around 97 % at 600 ppm of the extract and was observed the inhibitor acts as mixed-type of green corrosion inhibitor [21].

The las plant species are members of Rosaceae family and they have relationship by phytochemistry, it means share some biosynthesis pathways and formed related compounds. *Crataegus mexicana* (*C. mexicana*) belongs to the Rosaceae family, more specific is a member of Amydgaloidaea subfamily into this big family; and it is a beauty and high tree cultivated in Mexico and commonly known as tejocote (Figure 1), the name it was derived from a Nahuatl word Texocotl which means "acid and hard fruit". Mexico has 16 different tejocote species and they are endemic to this country, it means these species exist only in Mexico. The tejocote's fruits are eatable and in traditional medicine are used to treat respiratory system illness, the leaves and the cortex are used for digestive system and the roots are used as antidiabetic phytomedicine [22, 23]. Banderas-Tarabay et al., reported biological properties of interest and the antioxidant activity for *C. mexicana*, in which flavonoids can be highlighted [24, 25].

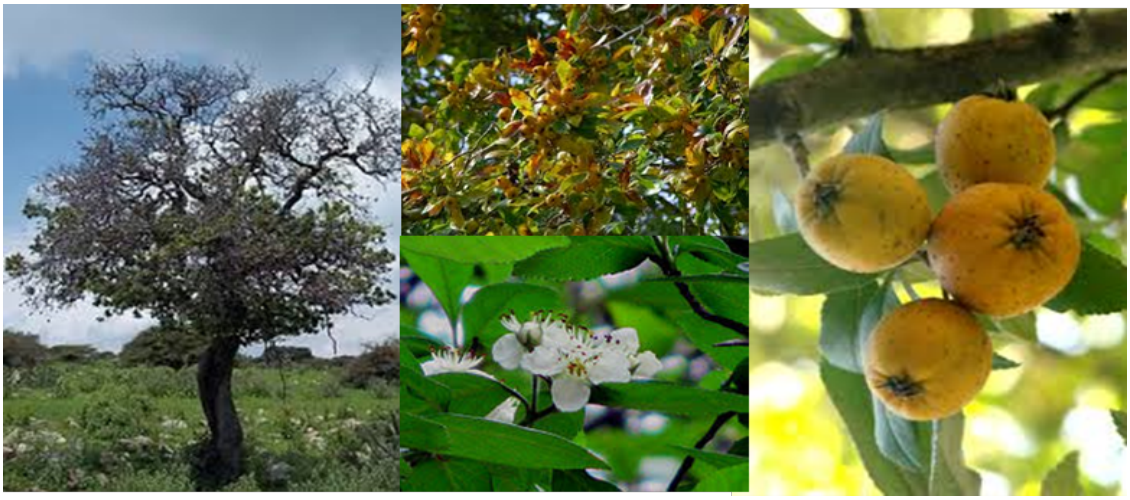

Figure 1.*Crataegus mexicana* (tejocote as common name).
Left: tree; Upper centre: leaves; lower centre: flowers; Right: Fruits

The tejocote's fruit and leaves contain many chemical compounds as presented in the Figure 2, flavonoids such as vitexina (1), quercetina (2) y rutina (3); oligomeric proanthocyanins, triterpene acids, organic acids, sterols and amines such as phenylethylamine (4), tyramine (5), isobutylamine (6) and acetylcholine (7) [26, 27]. These structures present N and O heteroatoms, as well the presence of π electrons (aromatic rings) which may have a good interaction with the metal surface. However, just the quercetin has been proved individually as corrosion inhibitor for Iron B500 in 1M of sulfuric acid through the electrochemical technique of EIS and potentiodynamic polarization curves obtaining a maximum efficiency of 59% [28]. Due to those antecedents the present research is about the study of *C. mexicana* as a corrosion inhibitor for AISI 1018 carbon steel in acid media.

2. Material and Methods

2.1. Preparation AISI 1018 carbon steel electrodes

The studied metal for the electrochemical tests was AISI 1018 carbon steel whose composition of weight percent is C 0.14-0.20%, Mn 0.60-0.90%, P < 0.040%, S < 0.050%, balance Fe. In order to obtain the samples, a cylindrical bar of AISI-1018 was cut in small pieces sized 2 cm in height X 0.6 cm in diameter, which were encapsulated in commercial epoxy resin joining the metal with a copper wire, which enables an electric contact, leaving an exposure area of 0.36 cm^2. Before every experiment, the metallic area was ground uniformly with SiC papers from 320 to 600 grain grades, washed with distilled water and degreased with acetone.

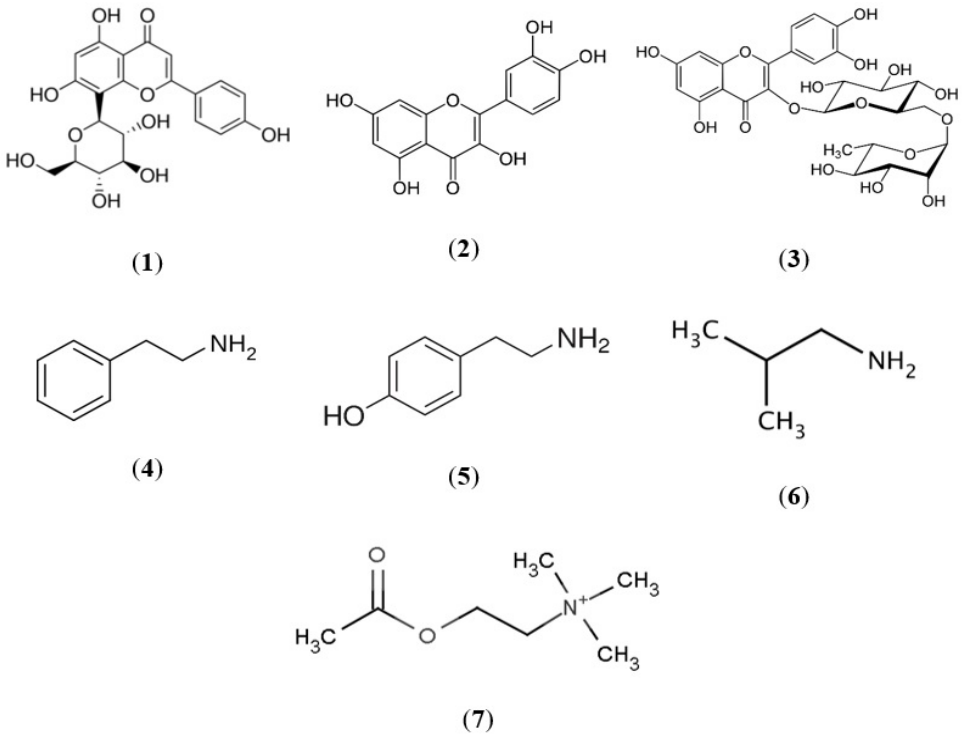

Figure 2. Chemical structures of some compounds present in *Crataegus mexicana*.

2.2. Eco-friendly corrosion inhibitor

C. mexica leaves were recollected at down town Tres Marias (at the coordinates Lat -99.241 / Lng 19.054) located in the municipality of Huitzilac, in the State of Morelos State, Mexico. The leaves were dried at room temperature (25 ºC ± 2) for three weeks in a dark chamber with natural aeration. Afterwards, the leaves were finely cut and exposed to a drying oven at 55 °C for 72 h. 500 g of dry leaves were macerated in a batch reactor using 1 L of methanol (99 %) at 25 °C and the reactor was protected against ultraviolet light, covering it with Aluminum fold and left at rest for 72 h. The obtained liquid mixture was filtered and the excess of solvent was evaporated using a rotary evaporator, producing 6 g of methanol *C. mexicana* extract, different concentrations of it in the ranged from 200 to 500 ppm were evaluated as eco-friendly corrosion inhibitor.

2.3. Electrolyte solution

The corrosive solution was made with sulfuric acid at 98% analytic grade and distilled water for preparing an aggressive solution of 0.5 M of H_2SO_4, evaluating different concentrations of *C. mexicana* (200-500 ppm).

2.4. Parameters of electrochemical tests

Electrochemical tests were carried out with a Potentiostat ACM instruments zero-resistance ammeter (ZRA) coupled to a personal computer, using a conventional glass cell with three electrodes. A graphite rod as counter electrode, a reference electrode Ag/Cl and a working electrode of AISI 1018 carbon steel. The electrodes were immersed in the aggressive solution with and with no inhibitor, around 10 minutes until reaching an open circuit potential stationary state (EOCP).

In order to determine the reproducibility each electrochemical experiment was done tree times. For the electrochemical impedance spectroscopy, the tests were made using a frequency interval between 10 KHz to 0.5 Hz obtaining 100 points per decade with amplitude of input sine-wave of ± 10 mV. For the potentiodynamic polarization curves a potential range used was between -300 to 400 mV around the corrosion potential and a scanning rate of 60 mV min^{-1} were applied.

2.5. Surface morphology analysis

The study of the surface morphology for the AISI 1018 carbon steel immersed in sulfuric acid without and with methanol extract of *C. mexicana* was carried out using a scanning electron microscope (SEM, Karl Seizz DSM100).

2.6. Chemical characterization of Eco-friendly corrosion inhibitor

The FT-IR analysis was realize using a Bruker IR spectrum model APLHA (Series TN: 301538) coupled to a work station equipped with the software Opus version 7.5, which is able to do the Fourier Transforms (FT) and then translate to an spectrogram. The sample was directly explored and measurement using a wave number range between 4000 to 400 cm^{-1}.

2.7. Toxicity test

Following the method proposed by Sobrero y Ronco [29], an evaluation of the phytotoxic effects of *C. mexicana* methanol extract through an acute toxicity bioassay using *Lactuca sativa* germinated seeds and the seedling growth. For such phytotoxic evaluation *L. sativa* seeds with pesticides free was used and obtained from Rancho los Molinos, Morelos, Mexico. 100 seeds were collocated inside a Petri box on a filter paper previously saturated with the different concentrations of the extract (200-500 ppm) with a positive control of 0.2M $ZnSO_4$ and a negative control with mineral water. Petri boxes were collocated in a hermetic bag for humidity preserving for 120 h with light absence and a constant temperature about (24 ± 2 °C). When the time was over, the germinated seeds were taken out and the lengths of the radicle and hypocotyl at the different concentrations were registered. All the tests were done three times to assure the reliability of the results.

3. Results and discussion

3.1. Potentiodynamic Polarization Curves

The performance of the *C. mexicana* as green corrosion inhibitor was evaluating on AISI 1018 carbon steel in acid media at room temperature was evaluated through potentiodynamic polarization curves to determine the mechanism and the kinetic in the anodic and cathodic reactions. The Figure 3 shows the polarization curves at different concentrations of the inhibitor. From these curves, it is observed how the Tafel anodic and cathodic slopes are affected in the presence of the inhibitor, reducing the rate of metal dissolution as well as retarding the hydrogen evolution reaction. This behavior indicates that *C. mexicana* is a mixed type inhibitor, cathodic prevailing [30]. The obtained parameters through polarization curves are shown in Table 1, which include the current density (I_{corr}) determined through Tafel extrapolation, the corrosion potential (E_{corr}), the corrosion rate (V_{corr}), the anodic (βa) and cathodic (βc) slopes and the extract inhibition percent (% EI), which was calculated through the Equation 1.

When the inhibitor is added, the corrosion potential E_{corr} is slightly displaced approximately 20 mV to more negative values accordingly to the blank, thus *C. mexicana* could be classified as a mix type inhibitor, which is preferentially absorbed in the metal cathodic zones [31].

$$\%EI = \left(\frac{I^0_{CORR} - I'_{CORR}}{I^0_{CORR}}\right) X100 \qquad \text{(Eq. 1)}$$

Where I^0_{CORR}, is the current density without inhibitor and I'_{CORR} is the current density with inhibitor.

Table 1. Values of electrochemical parameters from polarization curves.

[G-Inh]* (ppm)	βa (mV)	βc (mV)	I_{corr}(mA/cm^2)	V_{corr}(mm/year)	E_{corr} (mV)	% IE
0	64.95	120.63	1.59	18.45	-452.51	
200	65.183	128.63	1.03	12.03	-473.63	35
300	54.15	124.76	0.93	10.83	-465.98	41
400	57.84	147.57	0.79	9.64	-465.14	50
500	54.16	149.65	0.4	5.3	-472.71	75

*[G-Inh] Concentration of Green corrosion inhibitor

The current density decreased proportionally with the increase of the inhibitor concentration, indicating that inhibitor molecules are been absorbed onto the metal surface, avoiding that the aggressive species from the corrosive media reach the metal surface [32, 33]. This phenomenon causes that the corrosion rate decreases with the presence of the inhibitor and inhibitor efficiency raises, confirming that the oxidation-reduction reactions are

been affected due to the block of the active sites obtaining a maximum efficiency of 75% when the inhibitor is present in 500 ppm.

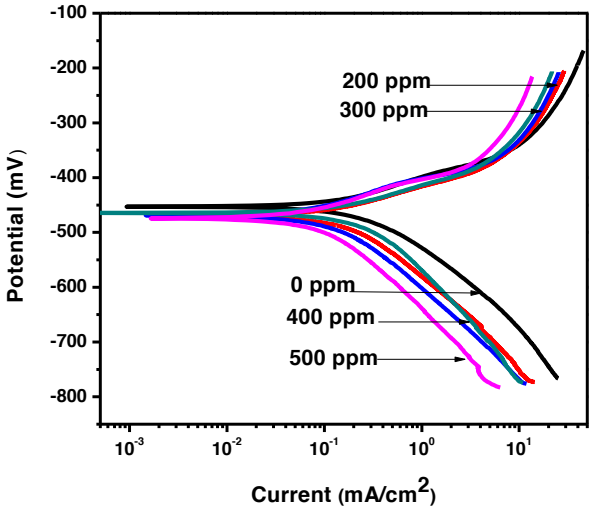

Figure 3. PPC of corrosion of AISI 1018 carbon steel in 0.5 M H_2SO_4 without and with *Crataegus mexicana*.

3.2. Electrochemical Impedance Spectroscopy

The effect of *C. mexicana* extract as corrosion inhibitor for the evaluation of AISI 1018 carbon steel in acid media was also studied by the EIS technique. In the Figure 4 the Nyquist and Bode diagrams for the different inhibitor concentrations together with the no inhibitor case are presented. From the Nyquist diagram, it can be observed a depressed semicircle with the center in the real axis. The deviation of the ideal semicircle is generally attributed to the frequency dispersion as well as the inhomogeneity of the metallic surface and to the mass transfer resistance [34, 35]. At low frequency values it is observed an inductive ripple, attributed to the interaction of two consecutive flows that constitute a two stage faradic process of adsorption in the pre-passivation potential range [36]. Also, it can be seen when the concentration of the inhibitor increases, the semicircle diameter increases indicating that the metal is protecting against corrosion.

Table 2. Values of electrochemical parameters from EIS of AISI 1018 carbon steel in 0.5 M H_2SO_4.

[EF-Inh]* (ppm)	R_s (Ωcm2)	R_{ct} (Ωcm2)	R_L (Ωcm2)	N	CPE (μf cm^{-2})	IE%
0	2.9	48	30	0.87	6.889E-05	0
200	5.6	84	12	0.86	4.306E-05	43
300	3.8	101	10	0.86	3.164E-05	52
400	6.8	153	13	0.85	3.024E-05	69
500	11	240	15	0.88	1.704E-05	80

*[EF-Inh] Concentration of Eco-friendly corrosion inhibitor

In the Figure 5 the equivalent circuit used to model the EIS results is presented for the corrosion system with and with no *C. mexicana* inhibitor. The Zview software was used to obtain the values shown in the Table 2: solution resistance (R_s), charge transfer resistance (R_{ct}), capacitance associated to a constant phase element (C_{PE}) used to substitute a double pure layer condenser and to model the deviation due an ideal capacitance. The ions solution migration resistance (RL) is associated to the inductance (L) at low frequencies observed at all inhibitor concentrations and the surface displacement (n), which is associated to non-ideal current distribution as a result of surface's roughness and other deficiencies [37]. The electrochemical double layer capacitance C_{dl} was calculated using the Equation 2.

$$C_{dl} = (2\pi f_{max} R_{ct})^{-1} \quad \text{(Eq. 2)}$$

Where f_{max} is the frequency at the maximum value of the imaginary impedance.

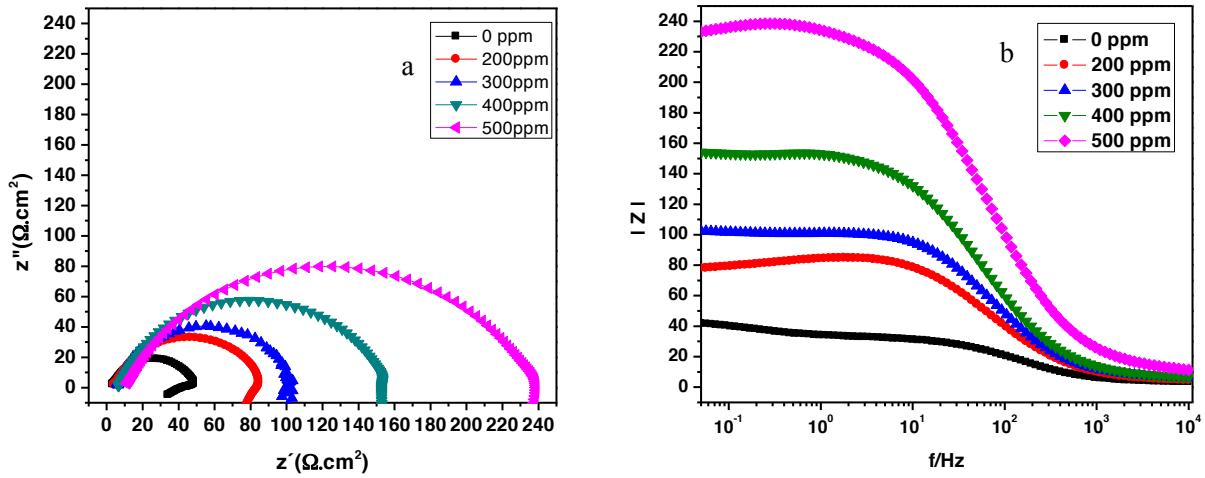

Figure 4. EIS of corrosion of AISI 1018 carbon steel in 0.5 M H_2SO_4without and with *Crataegus mexicana* a) Nyquist diagram b) Bode diagram.

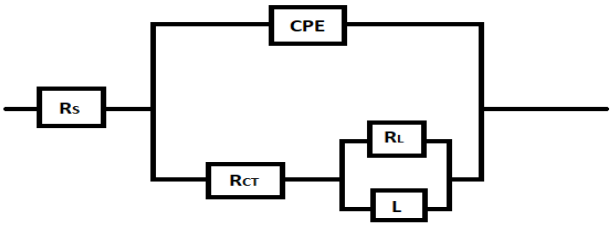

Figure 5. Equivalent circuit used to model EIS values of corrosion of AISI 1018 carbon steel in 0.5 M H_2SO_4 without and with *Crataegus mexicana*.

Results indicate that the double layer capacitance decreases as the inhibitor concentration increases, at the time that charge transfer resistance increases, as a result of the inhibitor adsorption onto the surface. The inhibitor molecules create a protective layer on the metal that prevents the interaction of the aggressive media with the metallic surface, therefore as the inhibitor concentration increases the thickness layer increases. This behavior agrees with the mentioned previously in the corrosion inhibitor for carbon steel using caffeic acid [38] and succinic acid [39]. The inhibitor efficiency reported in the Table 2 was calculated according to the Equation 3.

$$IE\% = \frac{R_{ct}^{'} - R_{ct}^{0}}{R_{ct}^{'}} \qquad \text{(Eq. 3)}$$

Where R_{ct}^{0} and $R_{ct}^{'}$ are the charge transfer resistances with and with no inhibitor respectively.

The corrosion inhibition efficiency increases directly with the inhibitor concentration increases, obtaining a maximum efficiency of 80% when was using 500 ppm of methanol *C. mexicana* extract. In the Figure 6 is observe the Nyquist diagrams from EIS for 500 ppm of Eco-friendly corrosion inhibitor at different residence time, is possible to observe that the semicircle diameters increase with the resident time increases and the charge transfer resistance also increases until 4h., reaching a maximum efficiency of 95%, which indicates that inhibitor molecules are absorbed onto the metal surface forming a protective layer, after 4 hrs., the protective layer becomes unstable, thus the charge transfer resistance begins to decrease[40].

3.3. Adsorption isotherms

The degree of surface coverage (θ) was calculated with the values of Inhibition efficiency the *C. Mexicana* eco-friendly corrosion inhibitor at the different concentrations according to the Equation 4.

$$\theta = \frac{EI}{100} \qquad \text{(Eq. 4)}$$

The adsorption characteristic of the *C. mexicana*eco-friendly corrosion inhibitor was also studied by fitting data obtained for the degree of surface coverage by three different models of adsorption isotherms,

Tempkin, Langmuir and Frumkin. The tests reveal that the adsorption for the inhibitor on the metal surface is best described by Frumkin adsorption isotherm. The assumptions of Frumkin adsorption isotherm can be expressed with the Equation 5:

$$log\frac{\theta C_{inh}}{1-\theta} = \log K + g\theta \quad \text{(Eq. 5)}$$

Where C_{inh} refers to the concertation of inhibitor, K is the desorption-adsorption equilibrium constant, and g correspond the parameter of adsorbate interaction.

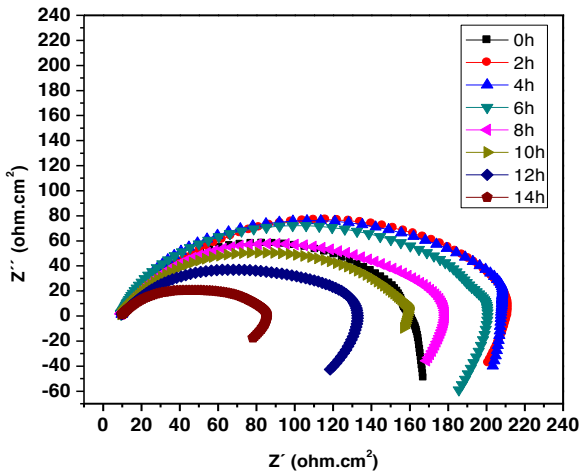

Figure 6. EIS of corrosion of AISI 1018 carbon steel in 0.5 M H_2SO_4 with *Crataegus mexicana* at different residence times

The plot of C/θ versus C straight line graph was obtained and is showing in the Figure 7, which proves that Frumkin adsorption isotherm is obeyed over the range of concentration studied. The values of the adsorption parameters of *C. Mexicana* eco-friendly corrosion inhibitor deduced from Frumkin plot are presented in the Table 3. For the obtained linear plot with which was calculated the adsorption constant (K_{ads}) as the inverse of slope and the Gibbs free energy was calculated with the Equation 6 [41] and the value, it is present in Table 3.

Table 3. Adsorption parameters deduced from Frumkin plot of *Crataegus mexicana* eco-friendly corrosion inhibitor

Slope	R^2	K_{ads}	$-\Delta G^0_{ads}$[kJ mol^{-1}]
2.9511	0.99	0.444	-7.94

$$\Delta G^0_{ads} = -RTln(55.5\ K_{ads}) \quad \text{(Eq. 6)}$$

Where R is the gas universal constant, T is the temperature in Kelvin grades, K_{ads} is the equilibrium constant of adsorption and 55.5 is the concentration of water in the inhibitor solution.

Some authors mentioned about the ΔG^0_{ads} values, and they say values around -20.0 KJ mol^{-1} or fewer negatives indicated physical adsorption where exists the attraction and repulse forces between inhibitor molecules and the metal surface. Values of ΔG^0_{ads} around -40.0 KJ mol^{-1} or more negative indicate a chemical adsorption processes derivate of the coordinative bonds formed between the inhibitor and the metal surface [21].

The ΔG^0_{ads} obtained for *C. Mexicana* eco-friendly corrosion inhibitor was -7.94 KJ mol-1, according to the literature this indicated that the adsorption process was through a physical interaction between inhibitor molecules and the metal surface. However, observing the resident time in that *C. mexicana* acts as eco-friendly corrosion inhibitor, is possible to mention that these interaction forces are little strong because *C. mexicana* acts as eco-friendly corrosion inhibitor during 4 h after this time the overall inhibition efficiency decreases. Adsorption isotherms and the immersion time, both are important parameters in assessing the stability of inhibitive behavior because the green corrosion inhibitors are degradable, they are not chemically like synthetic organic corrosion inhibitors, so their inhibition efficiencies are not occurring for long immersion times. Likewise is necessary to evaluate the immersion time for the green corrosion inhibitors and their influence on the inhibition efficiency in a period of time period since 2 from 24 h.

A few studies reported the residence time or the period of time when the green inhibitor acts. However, these periods could be considered shorts for green corrosion inhibitors but keep in mind the kind of aggressive

environment, the pH is different in salt solution than acid, such as *Prunus persica* green inhibitor on carbon steel in 0.5 M H_2SO_4 the residence time was 6 h [21] and for *Eucalyptus globulus* on C38 steel in sulfuric acid was the same time [42]; for *Medicago sativa* against carbon steel in 0.5 M H_2SO_4 the residence time was 8 h [43]; and for *Ricinus communis* the residence time reported was 2 h [44]. In this study the residence time was 4 h in with conserve the maximum corrosion inhibition efficiency was reached 80.00 %, by EIS at 500 ppm in 0.5 M H_2SO_4.

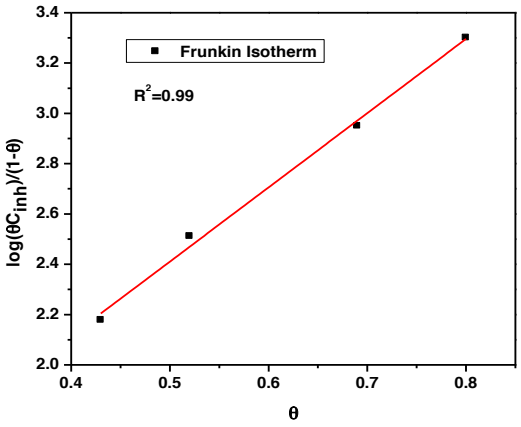

Figure 7. Frumkin adsorption isotherm from *Crataegus mexicana*eco-friendly corrosion inhibitor

3.4. Metal surface analysis

The surface morphology of AISI 1018 carbon steel immerse in 0.5M sulfuric acid in absence and presence of the methanol extract of *C. mexicana* was characterized. In order to demonstrate that at higher concentrations of the green inhibitor protected the metal surface and reduced the damage by acid corrosion. The imagens in the Figure 8 shows some micrographs corresponding to the surface samples of AISI 1018 carbon steel exposed to 0.5 M of H_2SO_4. In the Figure 8a is presented the image of the sample exposed without green inhibitor and after being immersed in the aggressive media for 4 h. It can be seen that the metal surface had the corrosion products before cleaned and after had a lot of cracks (Figure 8b) and it reveals a severe damage on the metal surface. The Figure 8c corresponds to the surface of metal immersed in the aggressive media and 500 ppm of green inhibitor in which what the maximum corrosion efficiency was registered.

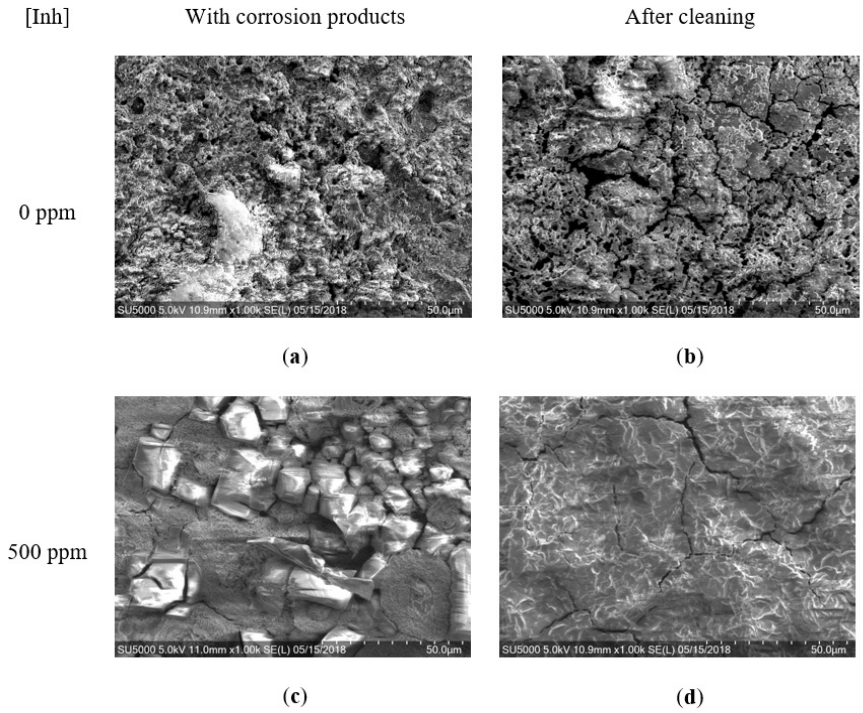

Figure 8. Micrographs of AISI 1018 carbon steel surface exposed to corrosion media without and with *Crataegus mexicana* as eco-friendly corrosion inhibitor.

It can be seen a compact layer with less porosity. After cleaned it is possible to observed (Figure 8d) without corrosion products on the metal surface less micro cracks and more regular metallic surface as consequence of the damage decreased. All this lead to observe that less damage on metal surface occurs with the green inhibitor presence.

3.5. Chemical characterization of green corrosion inhibitor

The methanol extract of *C. mexicana* was chemically characterized by FT-IR, was possible to observe the vibrations of the major functional chemical groups contained in the sample of green corrosion inhibitor. The FTIR spectrum (Figure 9) shows a set of significant vibrations at 3322 cm^{-1} is observed a wide and intense band characteristic of O-H bond of hydroxyl groups. At 2908 cm^{-1} is observed a coupled band of signals that evidences C-H bonds like $–CH_3$ and $–CH_2–$. An intense tight band at 1620 cm^{-1} proves evidence of existence C=O double bond from the carbonyl group vibration like ketone. At 1388 cm^{-1} an intense tight band of C-H bond reflection is seen, which can be assigned to methyl groups ($-CH_3$).

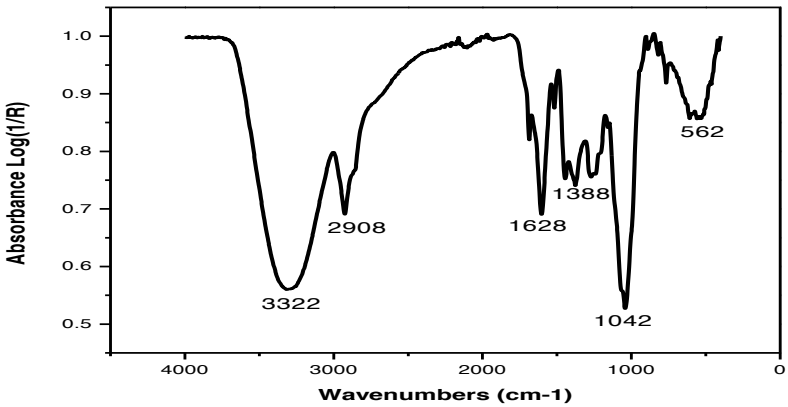

Figure 9. FT-IR spectrum of methanol extract of *Crataegus mexicana*

Also, a very intense and narrow signal at 1042 cm^{-1} confirms the vibration of C-O bonds, mainly alcohol. At 562 cm^{-1}, a wide and short signal is assigned to C-H bonds ($-CH_2-$). It is important to have in mind that flavonoids have carbon – carbon double bonds in their the aromatic ring structures, ketone carbonyls in ring C and secondary alcohols in rings A and B, as shown in the Figure 10. The result of FTIR analysis proved evidence of the presence of flavonoids in *C. Mexicana* eco-friendly corrosion inhibitor [45].

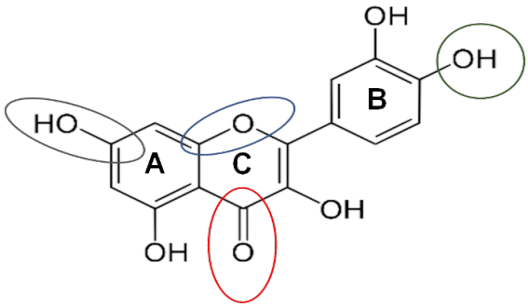

Figure 10. IR assignation of signals using a general chemical structure of flavonoid.
Green and blue C-O bond; Red C=O double bond and Brown O-H bond.

3.6. Toxicity text

The inhibition percent of the *Lactuca sativa* growth (% IL) was calculated using the Equation 7.

$$\% IL = \frac{\bar{x}t - \bar{x}e}{\bar{x}t} \quad \text{(Eq. 7)}$$

Where $\bar{x}t$ means growth of hypocotyl or radicle with the negative control (without eco-friendly corrosion inhibitor) and $\bar{x}e$ means growth in the presence of *C. mexicana*.

The Figure 11 it can be seen the *L. sativa* seedling growth inhibition graph at different concentrations of methanol *C. mexicana* extract. It is observed that when extract concentration is increased the inhibition percent

also increases, observing that that maximum inhibition of the radicle is of 42% whereas for the hypocotyl is of 39% using 700 ppm of the extract concentration.

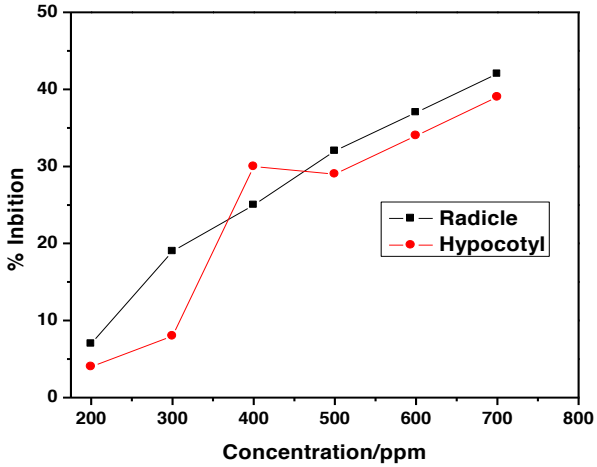

Figure 11. Inhibition percent curve for hypocotyl and radicle *L. sativa* seeds at different concentrations of methanol *Crataegus mexicana* extract.

The germination index (GI) was calculated using the Equation 8 [46].

$$GI\% = \frac{RSG*RGR}{100} \quad \text{(Eq. 8)}$$

Where RSG is the relative seed germination and RGR is the relative growth of the radicle.

In the Figure 12 is presented the germination index over 50 % of the population until the inhibitor concentration is above 700 ppm. According to the toxicity classification of released substances recommended in México by the Environment and Natural Resources Secretary (SEMARNAT by initials in Spanish), the Mexican Oil Institute (IMP by initials in Spanish) and the Ecology National Institute (INE by initials in Spanish) [47], is possible mentioned that *C. Mexicana* eco-friendly corrosion inhibitor can be classified as slightly toxic according *L. sativa* seeds bioassay because due to the concentration needed to cause damage effects in half the population is around 700 ppm, this value is consider into 500 to 5000 ppm average.

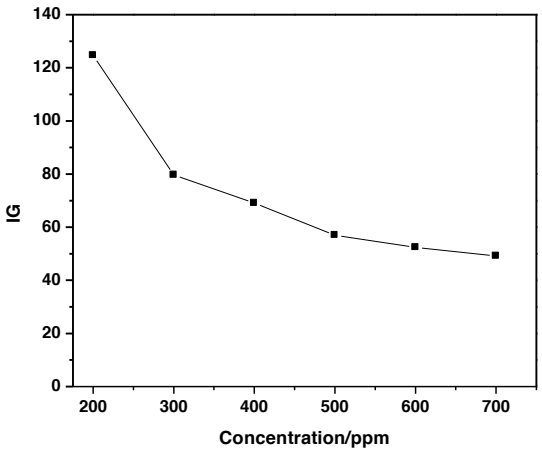

Figure 12. Hypocotyl and radicle germination index of *Lactuca sativa* using different concentrations of *Crataegus mexicana*

Conclusion

Through PPC was possible determined that the methanol extract *C. mexicana* acted as eco-friendly corrosion inhibitor mix type predominantly as cathodic type green inhibitor. 500 ppm of methanol*C. Mexicana* extract produced 75% as maximum corrosion inhibition efficiency by PPC. However through EIS tests, the

maximum corrosion inhibition efficiency was 80%. The weight loss method shown that after 4 h as immersion time the corrosion inhibition efficiency increased to 95% and then the corrosion inhibition decreases. The surface analysis lead to observe that less damage on metal surface occurs with the green inhibitor presence. The FTIR analysis showed the presence of flavonoids into the green inhibitor and the toxicity analysis with *L. sativa* seeds shown that methanol extract of *C. mexicana* could be result slightly toxic above 700 ppm as green inhibitor. All of these permitted to conclude that the performance of *C. mexicana* as eco-friendly corrosion inhibitor is adequate.

References

1. M. M. Solomon, S. A. Umoren, I. I. Udoroso, A. P. Udoh, *Corros. Sci.,* 52 (2010) 1317-1325.
2. G. Gao, C. Liang, *Eletrochim. Acta*, 52(2007) 4554-4559.
3. J. A. González Fernández, presented at Consejo superior de investigaciones científicas, Madrid, Spain, 1989.
4. T. Fallavena, M. Antonow, R. S. Gonçalves, Appl. Surf. Sci., 253 (2006) 566-571.
5. F.C. Giacomelli, C. Giacomelli, M.F. Amadori, V. Schmidt, A. Spinelli, *Mat. Chem. Phys*., 83(2004)124-128
6. F. S. De Souza, A. Spinelli, *Corros. Sci.,* 51(2009) 642-649.
7. N. Patel and G. Mehta, Green Corrosion Chemistry and Engineering: Opportunities and Challenges, Wiley-VCH VErlag& Co., Singapore, 2015.
8. G. I. Ramírez-Peralta, U. León-Silva, M. E. Nicho Díaz, M. G. Valladares-Cisneros, *Mater. Corros.,* 69 (2018) 1631-1637.
9. A. Bouoidina, F. El-Hajjaji, K. Emran, M. E. Belghiti, A. Elmelouky, M. Taleb, A. Abdellaoui, B. Hammouti, I. B. Obot. *Chem. Res. Chinese Universities*, 35 (2019) 85-100.
10. A. Salhi, I. Hamdani, A. Bouyanzer, N. Chahboun, H. Amhamdi, I. Warad, B. Hammouti, F. Bentiss, A. Zarrouk. *Anal. Bioanal. Electrochem*., 10 (2018) 1587-1610.
11. A. Ehsani, M. G. Mahjani, M. Hosseini, R. Safari, R. Moshrefi, H. Mohammad Shiri, *J. Colloid Interface Sci.,* 490 (2017) 444-451.
12. H. Bendaif, A. Melhaoui, A. Bouyanzer, B. Hammouti, Y. El Ouadi, *J. Mater. Environ. Sci.,* 8(2017)4475-4486
13. S. Bouazama, J. Costa, J. M. Desjobere, A. BenAli, A. Guenbour, A. Bellaouchou, A. Zarrouk and M. Tabyaoui, *J. Mater. Environ. Sci.,* 8 (2017) 2946-2955.
14. P.E. Alvarez, M.V. Fiori-Bimbi, A. Neske, S.A. Brandan, C.A. Gervasi, *J. Ind. Eng. Chem.,* 58(2018) 92-99.
15. G. Subramanian G, R. Sayee Kannan, M. Malarvizhi, P. Muthirulan, *JAEC,* 3(2017) 144-147.
16. E. Rodriguez-Clemente, J.G. Gonzalez-Rodriguez, M.G. Valladarez-Cisneros, J.G. Chacon-Nava, J.G. Flores-De los Ríos, L.M. Rodriguez-Valdez, *Journal of Materials and Environmental Science*, 8 (2017) 3817-3833.
17. E. Rodriguez-Clemente, J. G. Gonzalez-Rodriguez, M. G. Valladares-Cisneros, *Int J Electrochem Sci.*, 9 (2014) 5924-5936.
18. S. A. Umoren, Z. M., Gasem, & I. B. Obot, *Anti-Corros Methods and Materials*, 62 (2015) 19-28.
19. A. Rubaye, A. Abdulwahid, S. B. Al-Baghdadi, A. Al-Amiery, A. Kadhum, & A. Mohamad, *Int J Electrochem Sci.*, 10(2015)8200-8209.
20. R. S. Al-Moghrabi, A. M. Abdel-Gaber, H. T. Rahal. *IJIC*, 9 (2018) 255-263.
21. A. Rodríguez-Torres, O. Olivares-Xometl, M. G. Valladares-Cisneros, & J. G. González-Rodríguez, *Int J Electrochem Sci.*, 13 (2018) 3023-3049.
22. C. Monroy-Ortiz, P. Castillo España, Plantas medicinales utilizadas en el Estado de Morelos. 3th Edition, Universidad Autónoma del Estado de Morelos, Morelos, Mexico, 2010.
23. F. Geilfus, Enda-caribe, 1994, 257, Costa Rica.
24. J. A. Banderas-Tarabay, M. Cervantes-Rodriguez, M. Grada-Sanchez, M. Espindola-Lozano, E. Cuevas-Romero, A. Navarro-Ocana, D. Mendez-Iturbide, *Afr. J. Food Sci*., 9(2015) 208-222.
25. J. A. Balderas Tarabay, M. Cervantes Rodríguez, D. Mendez Iturbide *J Pharmacogenomics Pharmacoproteomics*, 6(2015) 153-160.
26. M. Benli, N. Yigit, F. Geven, K. Güney, Ü, Bingöl, *Cell Biochem. Funct.,* 26 (2008) 844-851.
27. D. Kumar, V. Arya, Z. Ali Bhat, N. Ahmad Khan, D. Nandan Prasad, *Rev Bras Farmacogn*., 22(2012) 1187-1200.
28. A. Çaçi, A. Lame, E. Kokalari, J. J. Zotaj, S. Cenolli, Conference Proceeding Book I, 2017, 90-94.
29. G. Castillo Morales, Ensayos toxicológicos y métodos de evaluación de calidad de aguas IMTA, 2004, 71-79, México.

30. M. Prabakaran, S. H. Kim, V. Hemapriya, M. Gopiraman, I. S. Kim, I. M. Chung, *RSC Advances*, 6(2016) 57144-57153.
31. P. Muthukrishnan, P. Prakash, B. Jeyaprabha, K. Shankar, *Arabian Journal of chemistry* 2015.
32. R. Idouhli, A. N´Ait Ousidi, Y. Koumya, A. Abouelfida, A. Benyaich, A. Auhmani, *International Journal of corrosion*, 2018, Article ID 9212705, 1-15.
33. K. Boumhara, M. Tabyaoui, C. Jama, F. Bentiss, *J. Ind. Eng. Chem*., 29 (2015) 146-155.
34. A. H. Seikh, E. M. Sherif, *Int. J. Electrochem. Sci.,* 10 (2015) 895.
35. H. H. Hassan, E. Abdelghani, M. A. Amin, *Electrochim Acta*, 52 (2007) 6359.
36. V. V. Elkin, A. I. Marshakov, A. A. Rybkina, M. A. Maleeva, *Russ J Electrochem.*, 47(2011) 136-146.
37. G. Moretti, F. Guidi, G. Grion, *Corros. Sci.,* 46(2004) 387-403.
38. F. S. de Souza, A. Spinelli, *Corros. Sci.,* 51(2009) 642-649.
39. M.A. Amin, S.S.A. El-Rehim, E.E.F. El-Sherbini, R.S. Bayoumy, *Electrochim. Acta*, 52(2007)3588-3600.
40. A. K. Singh, C. Gupta, E. E. Ebenso, *Int. J. Electrochem. Sci.,* 7 (2012) 11617-11633.
41. K. Rose, B. S. Kim, K. Rajagopal, S. Arumugam, & K. Devarayan, *J Mol Liq.,* 214 (2016) 111-116.
42. S. Rekkab, H. Zarrok, R. Salghi, A. Zarrouk, L. Bazzi, B. Hammouti, Z. Kabouche, R. Touzani, M. Zougagh, *JMES*, 3(2012) 613-627.
43. A. Rodríguez Torres, M.G. Valladares Cisneros, J.G. González Rodríguez, *Green Chem Lett Rev,* 9(2016) 143-155.
44. A. D. M. Santos, T. F. D. Almeida, F. Cotting, I. V. Aoki, H. G. D. Melo, & V. R. Capelossi, *Mat Res,* 20(2017)492-505.
45. R. Nunes Oliveira, M. Cordeiro Mancini, F. Cabral Salles de Oliveira, T. Marques Passos, B. Quilty, R. M. da Silva Moreira Thiré, G. B. McGuinness, *Matéria*, 21(2016) 767-779.
46. F. Zucconi, A. Pera, M. Forte, M. de Bertoldi, *Bioclycle*, 22 (1981) 54-57.
47. L.C. Fernández Linares, N.G. Rojas Avelizapa, T.G. Roldán Carrillo, M.E. Ramírez Islas, H.G. Zegarra Martínez, R. Uribe Hernández, R.J. Reyes Ávila, D. Flores Hernández, J.M. Arce Ortega, Manual de Técnicas de análisis de suelos aplicadas a la remediación de sitios contaminados. Instituto Mexicano del Petróleo, Secretaría de Medio Ambiente y Recursos Naturales Instituto Nacional de Ecología, México, 2006

(2019) ; http://www.jmaterenvironsci.com